BIBECHANA
Vol. 20, No. 3, December 2023, 224–235

ISSN 2091-0762 (Print), 2382-5340 (Online)
Journal homepage: http://nepjol.info/index.php/BIBECHANA
Publisher:Dept. of Phys., Mahendra Morang A. M. Campus (Tribhuvan University)Biratnagar

Enhanced electronic and magnetic performance of MoS_2 monolayer via Tc & Nb impurities defect and water adsorption on impurities defected materials

Hari Krishna Neupane[1,**], **Prakash Khatri**[2], **Arun Devkota**[2]
Narayan Prasad Adhikari[2,*]

[1]*Amrit Campus, Institute of Science and Technology Tribhuvan University,* Kathmandu, Nepal
[2]*Central Department of Physics, Institute of Science and Technology,* Tribhuvan University, Kathmandu, Nepal

[*]Corresponding author. Email: narayan.adhikari@cdp.tu.edu.np
[**]Email: hari.neupane@ac.tu.edu.np

Abstract

This study examined the effect of Tc & Nb impurity atoms on MoS_2 (Tc-MoS_2 & Nb-MoS_2), and adsorption of water molecule on impurities defected MoS_2 (Tc-W-MoS_2 & Nb-W-MoS_2) material from first-principles calculations. By the estimation of their ground state energy and binding energy, they are stable 2D materials. From band structure and density of states (DoS) calculations, Tc & Nb impurities affect the nature of pristine MoS_2. It is found that Tc-MoS_2 has n-type & Nb-MoS_2 has p-type semiconducting nature. Water interaction on Tc-MoS_2 & Nb-MoS_2 slightly changes the electronic properties and impacts the bandgap, which enhanced the electronic performance of material than that of pristine MoS_2. The magnetic properties of Tc-MoS_2, Nb-MoS_2, Tc-W-MoS_2, and Nb-W-MoS_2 are analyzed and found to exhibit an uneven distribution of up-spin and down-spin states of electrons in the orbital of atoms near the Fermi level. It reflects that they have magnetic properties. The non-magnetic MoS_2 material changes in to weak magnetic defected-MoS_2 materials due to the presence of Tc, Nb and adsorbed water molecule. It means, impurity defects add to magnetic properties of pristine MoS_2. Magnetic properties on defected MoS_2 occurred due to the dominant contributions of spin states of 4d-orbital of Mo, Tc, Nb atoms, and 3p-orbital of S atoms in the structures. This study highlights the impact of Tc & Nb impurity atoms and adsorbed water molecule on impurities defected MoS_2. The studied materials have potential applications in the fields of catalysis, nanoelectronics, biomedicine, and magnetic sensors on the basis of their electronic and magnetic properties.

Keywords
Adsorption, Defect, Fermi, Impurity, semiconducting.

Article information
Manuscript received: August 10, 2023; Accepted: September 1, 2023
DOI https://doi.org/10.3126/bibechana.v20i3.57470

1 Introduction

Two-dimensional (2D) transition-metal dichalcogenides (TMDCs) are a type of compound that consists of a transition metal from group IV-X (e.g., Mo or W) and a chalcogen element (S, Se, or Te) arranged in the form MX_2 [1]. These compounds can have a variety of properties, including metallic (such as VS_2 and NbS_2), semiconducting (such as $MoS_2$and WS_2), or insulating (like HfS_2) [2, 3]. TMDCs have a structure where one layer of M atoms is sandwiched between two layers of X atoms, and these layers are held together by van der Waals (vdWs) force. Their structure is composed of a honeycomb pattern [4, 5]in which the three atomic planes (chalcogen-metal-chalcogen) stack to create the individual layers of the material [6]. The MoS_2 monolayer is a semiconducting TMDs material that has Mo and S atoms stacked together in an S-Mo-S configuration, which results in a direct bandgap of 1.80 eV [5–9]. The unique properties of hexagonal TMDs materials include their atomic-scale thickness as well as their direct bandgap in its electronic band (wide bandgap exotic semiconductor), which can vary depending on the stacking order [3, 7, 10]. The weak interlayer forces, strong spin-orbit coupling, and robustness of MoS_2 make it an attractive material for electronic and mechanical applications due to its layered structure [11–13]. Due to its high on/off current ratio and higher carrier mobility at room temperature, MoS_2 has applications in field-effect transistors (FETs) and photodetectors [14, 15]. 2D semiconductors, both in the form of monolayer and multilayer, have a wide range of applications. They include usage in transistors, signal amplifiers and integrated logic circuits [16]. They also have potential uses in photocatalysts, solar cells, spintronics, flexible optoelectronics, nanoelectronics, nanophotonic, nanosensing, energy harvesting, photovoltaic solar cells, photocatalytic cells [17–19], DNA sequencing, biological and chemical sensors, lubricants, and catalytic surfaces for hydrogen storage in technology and industrial sectors [20, 21].

The electronic properties of 2D materials can be affected by external factors such as strain, electric field, pressure, temperature, doping, and defects. This means that the properties of TMDCs can be adjusted by controlling the environment they are in [22–25]. It is interesting to study how 2D materials like TMDCs interact with various solvents, such as water, due to their atomically flat surfaces which allow for different hydrophobic and long-range interactions [26, 27]. The areas around the edges and vacancies in 2D materials are highly sensitive to the adsorption of molecules, which can change the electronic and magnetic properties of the layers by distorting their arrangement [24, 28]. The way that H_2O interacts with MoS_2 can vary depending on where it is adsorbed [29]. The way that 2D materials interact with other materials, biomolecules, solvents and ions is affected by the structure of water at the interface [30–32]. The ability to tune the electronic structure of 2D-TMDs is made possible by the strong relationship between defects and chemical dopants in these materials, as well as the stacking of multiple monolayers [33, 34]. MoS_2 based devices are used in moisture environment too, so MoS_2-based devices can also be used in moist environments. However, the adsorption of water molecules on the monolayer MoS_2 can lead to water-induced oxidation and the formation of Molybdenum Trioxide (MoO_3), which causes the loss of lubricity [35, 36]. Various studies have revealed that the accumulation of hydrocarbon contaminants in the air can cause MoS_2 to become more hydrophobic over time, and this can affect the material's electrical or structural properties [37]. Despite the amount of research on the interaction of MoS_2 with water, the interactions of impurity-defected MoS_2 with water have not been thoroughly examined. Understanding these interactions could lead to the development of more efficient 2D materials-based biological and chemical sensors for medical devices [38].

Crystalline structures inevitably contain defects, or deviations in the arrangement of atoms or ions, and are considered a necessary consequence of entropy considerations in solids [39, 40]. Imperfections in solid materials, such as the replacement of an atom with a foreign atom or the removal of an atom from the structure, are known as impurity and vacancy defects respectively. These defects play a crucial role in altering and utilizing the undesired properties of the material [41]. These defects can lead to the discovery of new electronic, magnetic, mechanical, and transport properties in materials. This can have potential applications in various fields including catalysis, nanoelectronics, biomedicine, magnetic sensors, and more. It is crucial to study the properties of 2D materials with defects and how they are affected by these imperfections [42, 43].

Previous studies have investigated the structural, electronic and magnetic characteristics of a pure MoS_2 monolayer [8, 9], but the effect of impurities such as Tc, Nb on MoS_2 and water absorbed on impurities defected MoS_2 have not been reported. The current study aims to examine the impact of the impurity atoms on MoS_2 using first-principles calculations that combine spin-polarized density functional theory (DFT) method. The remainder of the paper is structured as follows: the methodology and computational details used in the study are discussed in Section 2, the findings, results and discussion are presented in Section 3, and the final conclusions of the work are outlined in Section 4.

2 Methods and Mateials

The study carried out structural optimization, electronic and magnetic properties calculations using density functional theory (DFT) method [44] implemented in the Quantum ESPRESSO code [45] using ultra-soft pseudopotentials (USPPs). The Grimme model of USPP suggests the use of the Rappe-Rabe-Kaxiraas Joannopoulos (RRKJ) model to describe weak van der Waals (vdWs) interactions in the system. This model of USPPs includes only the chemically active valence electrons in the calculations, which reduces the complexity of the effects caused by the motion of non-valence electrons of an atom and its nucleus [46]. The valence electronic configuration in H, C, Mo, O, S, Tc and Nb atoms of our system are H: $1s^2$; O: [He] $2s^2 2p^4$; S: [Ne] $3s^2 3p^4$; Mo: [Kr]$4d^5$ $5s^1$; Tc: [Kr] $4d^5$ $5s^2$ and Nb: [Kr] $4d^5 s^1$ respectively. We used a (3×3) supercell structure of monolayer MoS_2 to perform our calculations. First, we created the unit cell of MoS_2 using the XCrySDen (structure visualization software) and Quantum ESPRESSO (QE) computational tools. We have used an experimental lattice parameter of value 3.19 Å in the input file. We then converged the kinetic energy cut-off value, k-points, and lattice parameters. We then constructed impurity defects in MoS_2 by replacing the central Mo atom with Nb and Tc respectively and then water molecule adsorbed on impurity defected MoS_2 are shown in Fig. 1(a-d) respectively. The study also used a plane wave basis set and generalized gradient approximation (GGA) with Perdew, Burke, and Ernzer (PBE) to incorporate electronic exchange and correlation (XC) potential in the calculations [47]. The plane wave basis set is used to implement kinetic energy cutoff and charge density cutoff in the calculations. The kinetic energy cutoff used is 35 Ry and the charge density cutoff is 10 times the kinetic energy cutoff, which is 350 Ry, for all systems using USPPs for plane wave expansion. A (8×8×1) k-mesh generated using the Monkhorst-Pack (M-P) scheme is used to integrate the Brillouin Zone (BZ) during self-consistent calculations and structure optimization in the first irreducible Brillouin Zone [48, 49]. The calculations are stopped when the total energy and force reached a threshold of 10-4 Ry and 10-3 Ry/Bohrs respectively to ensure accurate results. The optimization of all structures is done using the Broyden-Fletcher-Goldfarb-Shanno (BFGS) [50] algorithm until the change in total energy is less than 10-4 Ry and the force is less than 10-3 Ry/Bohrs between two consecutive scf iterations. The calculations used a small broadening width of 0.001 Ry using the Marzarri-Vanderbilt (M-V) smearing method to ensure the accuracy of the results [51]. The "david" diagonalization method with a mixing factor of 0.6 is chosen for self-consistency. In order to study magnetic properties, spin-polarized density of states (DoS) and partial density of states (PDoS) calculations are performed. The systems are relaxed by using optimized values of kinetic energy cutoff, charge density cutoff, k-points, and lattice parameters. The self-consistent total energy calculations are done after the relaxation. The band calculations are done by selecting 100 k-points along the high symmetry points in the reciprocal lattice. These k-points are the sampling points in the first Brillouin Zone of the reciprocal lattice. Before calculating the density of states (DoS) and partial density of states (PDoS), non-self-consistent (nscf) calculations are done using an automatic denser mesh of (16×16×1) k-points, with a verbosity setting of "high" and an occupation setting of "tetrahedra".

3 Results and Discussion

In this section, we discussed in detail about the structural, electronic, and magnetic properties of pristine MoS_2, Tc & Nb impurities defected MoS_2 materials, and water adsorption on impurities defected MoS_2 materials. The analysis is based on spin-polarized DFT method of calculations.

3.1 Structural Analysis

In this section, we have discussed the structural properties of pristine MoS_2, Nb & Tc impurities defected MoS_2, and water adsorbed on impurities defected MoS_2 materials. Firstly, we have prepared unit cell of MoS_2 and check its stability by calculating its ground state energy and binding energy, it is found to be stable 2D material. After that, we have prepared (3×3) supercell structure of MoS_2 by extending unit cell along x-and y-axis, which is used for further calculations. So, we examined the stability of (3×3) supercell structure of MoS_2 by estimating its ground state energy -1741.61 Ry and binding energy 6.83 eV, and found that it is stable material. This estimated binding energy value is comparable with reported value of other stable 2D materials [52, 53]. The binding energy of MoS_2 is found by using equation (1) [24];

$$(E_b)_{Mo-S2} = [E_{MoS2} - NE_{Mo} - N'Es]/N" \quad (1)$$

where, $(Eb)_{Mo-S2}$ is the binding energy per Mo-S_2 pair, E_{MoS2}, E_{Mo} & E_S are the ground state energy of MoS_2, single Mo & single S atoms respectively, N & N' respectively represent the number of Mo atom & S atom present in supercell structure, N" indicates the total number of atoms present in supercell structure. Moreover, we have constructed Tc impurity defected MoS_2 ($Tc\text{-}MoS_2$) material by replacing Mo sites atoms from stable (3×3) supercell structure of MoS_2, and then relax calculations are done. The minimum ground state energy of value -1774.07 Ry and maximum binding energy of value 7.32 eV are obtained at the center position of Mo atom of Tc-MoS_2, is shown in Fig. 1(a). This value is close with reported value of other 2D materials [52, 53]. Similar procedure is done for the fabrication of Nb impurity defected MoS_2 supercell structure (Nb-MoS_2). The estimated ground state energy and binding energy of Nb-MoS_2 are found to be -1711.97 Ry & 6.42 eV respectively. The estimated binding energy of Nb-MoS_2 agrees with reported value of other 2D martials [52, 53]. Hence, Nb-MoS_2 is a stable 2D material, is shown in Fig. 1(b). The binding energy of Tc-MoS_2 and Nb-MoS_2 are obtained by using equation (2) [24];

$$(E_b)_{Tc/Nb-Mo-S2} = \left[E_{Tc/Nb-MoS2} - NE_{Mo} - N'E_S - N''E_{Tc/Nb}\right]/N''' \quad (2)$$

where, $(E_b)_{Tc/Nb-Mo-S2}$ is the binding energy per Tc-MoS2 pair, $E_{Tc/Nb-MoS2}$, E_{Mo}, $E_{Tc/Nb}$ & E_S are the ground state energy of Tc/Nb-MoS2, single Mo, single Tc or Nb & single S atoms respectively, N, N' & N" respectively represent the number of Mo atom, number of S atom, and number of Tc or Nb atom present in impurities defected MoS_2 supercell structure, N"' denotes total number of atoms present in defected supercell structures.

Furthermore, water molecule is adsorbed on different positions at 2.45 distance above the surface of Tc-MoS_2 & Nb-MoS_2, it is found that adsorbed water molecule (i.e., physio-adsorption) is at 2.45 distance vertically from the center position of MoS_2 are more stable materials, which are shown in Fig. 1(c-d). This is because they have minimum ground state energies (-1810.08 Ry of Tc-W-MoS_2 & -1747.98 Ry of Nb-W-MoS_2 respectively), and maximum binding energies (7.89 eV of Tc-W-MoS_2 & 6.98 eV of Nb-W-MoS_2 respectively) than other positions of adsorbed water molecule on defected MoS_2. These binding energies are fairly agree with reported value of other stable 2D materials [52, 53]. We have also estimated the adsorption energy of water molecule with Tc-MoS_2 & Nb-MoS_2 by using equation (3), and found to be 2.17 eV & 2.08 eV respectively. They are comparable with the reported values of water adsorption on 2D materials [9, 25, 27]. Hence, water adsorbed defected materials are stable 2D materials.

$$E_a = E_{Tc/Nb-MoS2} + E_{H2O} - E_{Tc/Nb-W-MoS2} \quad (3)$$

where, E_a is the adsorption energy of water molecule with Tc-MoS_2 or Nb-MoS_2 materials, $E_{Tc/Nb-MoS2}$ & E_{H2O}, are the ground state energy of Tc-MoS_2 or Nb-MoS_2 and adsorbed water molecule respectively. From the estimation of binding energies of Tc-MoS_2, Nb-MoS_2, Tc-W-MoS_2 and Nb-W-MoS_2 materials, we concluded that Tc impurity defected MoS_2 are more compact than Nb impurity defected MoS_2 structure.

3.2 Electronic and Magnetic Properties

Solid materials are made up of a large number of atoms, each with discrete energy levels for their electrons. When two similar atoms are brought together, their atomic orbitals overlap and split into distinct energy levels for the molecule, forming a continuous range of energy known as an energy band. Understanding the band structure and density of states (DoS) of a solid material provide insight into its electronic properties. Magnetic properties of materials are explored by analyzing of their density of states (DoS) and partial density of states (PDoS). Therefore, electronic and magnetic properties of Tc & Nb impurities defected MoS_2 materials (Tc-MoS_2 & Nb-MoS_2), and water adsorbed on Tc & Nb impurities defected MoS_2 materials (Tc-W-MoS_2 & Nb-W-MoS_2) are studied by analyzing their band structure, DoS and PDoS plots. The band structures of Tc-MoS_2, Nb-MoS_2, Tc-W-MoS_2 and Nb-W-MoS_2 are shown in Fig. 2(a-d) respectively.

To understand the electronic properties of Tc-MoS_2, Nb-MoS_2, Tc-W-MoS_2 and Nb-W-MoS_2 materials, band structure and DoS calculations are performed. For that, we have chosen first Brillouin Zone of the reciprocal lattice. The x-axis of the band structure plot represents the high symmetric points Γ-M-K-Γ of the first Brillouin Zone, with the -center being one of these points, and the y-axis corresponds to energy values. A total of 100 k-points are selected along these high symmetry points, which define a sampling path and irreducible region within the Brillouin Zone. In an ideal condition where the crystal is not under non-uniform strain or has imperfections. The repetition of the sampling path will cover the entire space of the Brillouin Zone. The band structure diagrams also have a horizontal dotted line, which represents the Fermi energy level. As seen in the band structure of Tc-MoS_2, band states of conduction band are moving closer to the Fermi energy level than that of valence band due to the rearrangement of spin states of electrons in the 3s, 3p orbitals of S atoms with 4d, 5s orbitals of Tc atom in structure. Hence, number of charge carriers in conduction band are greater than that in the valence band. It reveals that Tc-MoS_2 is a n-type semiconducting material having direct bandgap energy 1.01 eV at

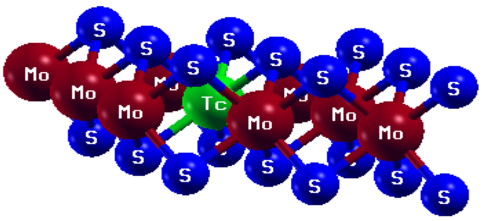

(a)

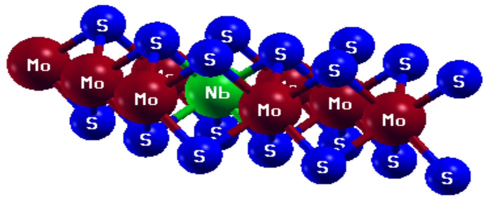

(b)

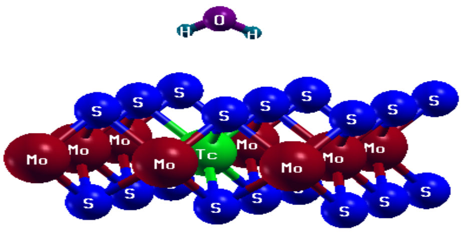

(c)

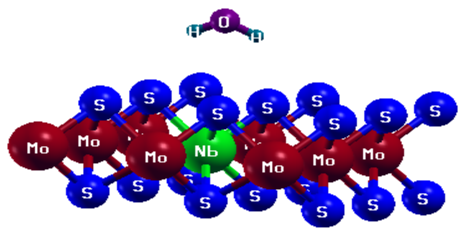

(d)

Figure 1: (Colour online) Supercell structure of (a) Tc impurity defect on MoS_2 (Tc-MoS_2), (b) Nb impurity defect on MoS_2 (Nb-MoS_2), (c) water adsorbed on Tc impurity defected MoS_2 (Tc-W-MoS_2), and (d) water adsorbed on Nb impurity defected MoS_2 (Nb-W-MoS_2).

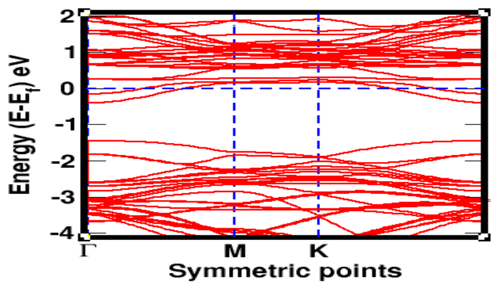

(a)

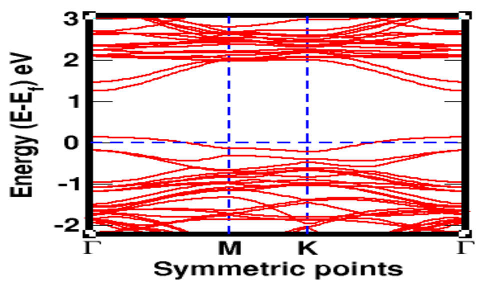

(b)

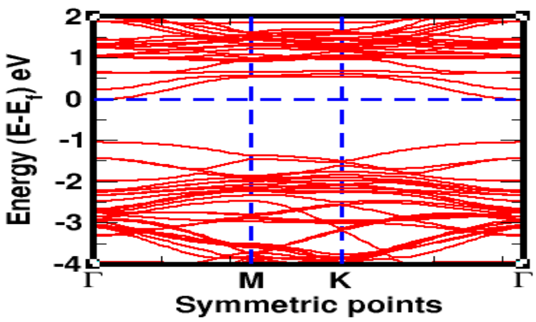

(c)

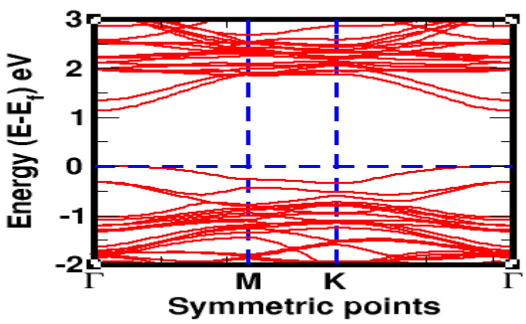

(d)

Figure 2: (Colour online) band structure plots of; (a) Tc-MoS_2, (b) Nb-MoS_2, (c) Tc-W-MoS_2 and (d) Nb-W-MoS_2. In figures, the horizontal dotted line represents the Fermi level, and the vertical dotted line intersects at high symmetry points.

Γ-point. This result is deviating from the properties of pristine MoS_2 [5–7], due to the presence of Tc impurity defects. We have estimated the bandgap energy of Nb-MoS_2 material by the analysis of it band structure calculations and found direct bandgap energy 1.10 eV in between the conduction band minima and valence band maxima at high symmetry Γ-point. Band states of valence band lies closer to the Fermi energy level than the band states of conduction band. This is because unpaired arrangement of spin states in the 3s, 3p orbitals of S atoms with 4d, 5s orbitals of Nb atom in structure. We concluded that Nb-MoS_2 is a p-type semiconductor material. This property is different than of pure MoS_2 [6,7], which is attributed due to the presence of Nb impurity defects in Nb-MoS_2. We have also analyzed the density of states (DoS) plots of Tc-MoS_2 & Nb-MoS_2 materials are shown in Fig. 3(a-b) respectively. It is found that distributed up-spin and down-spin states open bandgap energy due to the presence of unpaired spin states in the orbital of Tc & Nb atoms with S atoms respectively in structures. It also confirmed that Tc-MoS_2 is a n-type and Nb-MoS_2 is a p-type semiconductor material. From the analysis of above calculations, we concluded that impurity defects enhanced the electronic conductivity in materials. Semiconducting materials have wide applications due to their reliability, compactness and low cost; they are having probable future. Thus, p-type and n-type semiconductors find a wide variety of applications in the fields of memory, sensing, electronic, spintronic, optoelectronic devices [38, 42, 43].

Electronic properties of material are affected due to presence of moisture [25, 32]. So, we have investigated the electronic properties of water adsorbed on impurities defected MoS_2 through band structure and DoS plots. The band structures of Tc-W-MoS2 & Nb-W-MoS_2 are shown in Fig. 2(c-d) respectively. In the band structure of Tc-W-MoS_2, a direct bandgap of 1.13 eV is observed at -point. Its Fermi energy level being closer to the conduction band, which indicates that Tc-W-MoS_2 exhibits n-type semiconductor. The bandgap energy of Tc-W-MoS_2 has slightly greater value than that of Tc-MoS_2 material because adsorbed water molecule reduces binding energy (losses lubricity). It is observed that band states are slightly repelled towards conduction band from Fermi energy level in band structure is shown in Fig. 2(c). This is also confirmed by the analysis of its DoS plot is shown in Fig. 3(c). In DoS plot, bandgap energy is computed in between upper level of valence band and lower level of conduction band of distributed up- and down-spin states of electrons in the orbital of atoms present in the material. Furthermore, we have computed the bandgap energy of Nb-W-MoS_2 material on the basis of band structure and DoS plots, are shown in Fig. 2(d) & 3(d) respectively. The band structure of Nb-W-MoS_2 reveals a direct band gap of 1.23 eV at Γ-point, which coupled with the Fermi energy being positioned near the valence band, indicates that Nb-W-MoS_2 has p-type of semiconducting properties. This obtained result is slightly deviated from the semiconducting behavior of pure MoS_2, which is due to the presence of adsorbed water molecule and Nb impurity defect on MoS_2. To confirm the predicted nature of Nb-W-MoS_2, we have analyzed the DoS of it and found that distributed up- and down-spin states are appeared near the valence band is shown in Fig. 3(d). This confirmed that it has p-type semiconducting properties. Water molecule can interact with impurities, altering their electronic and chemical states and subsequently modifying the band structure, and hence inflate the electronic properties than that of pristine MoS_2. Additionally, water adsorbing on the surface of MoS_2 can form a thin layer of water molecules and influence the electronic properties of the material. This can result in the creation of new energy levels leading to new electronic states and modifications to the bandgap energy.

Effect of impurities (Tc & Nb) defect on pristine MoS_2 and adsorbed water molecule on impurities defected MoS_2 initiate to switch in band structures and DoS plots. As a result, Fermi energy, Fermi shift, total ground state energy, bandgap energy, and binding energy of defected materials have changed than that of pristine form, they are presented in Table-1. The reason of shifting band states in band and DoS from pristine to defected systems are; H atom has one unpaired up-spin electron in 1s orbital, O atom has paired spins in 2s orbital and paired electrons in $2p_x$ sub-orbital, and unpaired electrons in $2p_y$ and $2p_z$ sub-orbitals. The Mo atom has one unpaired up-spin electron in 5s orbital and one in 4d orbital with sub-orbitals $4d_{xy}$, $4d_{xz}$, $4d_{yz}$, $4d_{x^2-y^2}$, $4d_{z^2}$. Tc atom has paired spins in 5s orbital and one unpaired up-spin electron in $4d_{xy}$, $4d_{xz}$, $4d_{yz}$, $4d_{x^2-y^2}$ & $4d_{z^2}$ sub-orbitals. Nb atom has one unpaired up-spin electron in 5s orbital, one unpaired electron in $4d_{xy}$, $4d_{xz}$, $4d_{yz}$ & $4d_{x^2-y^2}$ and one vacant in $4d_{z^2}$ sub-orbital. The S atom has paired spins in $3p_x$ sub-orbital and one unpaired up-spin electron in $3p_y$ & $3p_z$ sub-orbitals. These different electronic configurations affect the electronic and magnetic properties of materials.

The magnetic properties of materials can be evaluated by analyzing their density of states (DoS) and partial density of states (PDoS). These plots provide insight into the distributions of electrons with up- and down-spins within the material. When the distributions are symmetrical, meaning that the number of up- and down-spins of electrons are equal, magnetic moments of the electrons canceled out, resulting in non-magnetic properties. However, when the distributions are asymmetrical, there are more up- or down-spins of electrons, it leads to a net magnetic moment, resulting in magnetic properties. This occurs when electrons of the atoms are not paired, meaning the presence of unpaired up- and down-spins of electrons in the atomic orbitals create certain magnetic moment, leading to magnetic properties of the material. In other words, the DoS and PDoS calculations of spin-polarized systems reveal the distributions of electrons with opposite spins in the material. If the number of electrons with opposite spins are equal, the material is non-magnetic. But, if the distributions are asymmetrical, the material has magnetic properties. The reason is that electrons with opposite spins can pair up, which cancels out their magnetic moments. But, if there are more electrons with one spin direction, the material will have a net magnetic moment, making it magnetic. The PDoS plot of Tc-MoS_2, Nb-MoS_2, Tc-W-MoS_2 and Nb-W-MoS_2 are presented in Fig. 4(a-d) respectively.

DoS plots (Fig. 3(a-d)), and PDoS plots (Fig. 4(a-d)) come up with the information's of distributed spin states in electronic orbitals of atoms present in the materials. The DoS plots of considered materials give insight into how the impurities and adsorbed water molecule affect the electronic and magnetic properties of MoS_2. Hence, DoS used to understand how the defects and adsorbed water molecule influenced the electronic and magnetic properties of materials. The detail investigation of magnetic properties of Tc-MoS_2, Nb-MoS_2, Tc-W-MoS_2 and Nb-W-MoS_2 materials, we have analyzed PDoS plots. In PDoS analysis, we especially focused the impact of distributed electronic spin states in the orbitals of atoms present in the materials. It shows how the electrons are spread among different orbitals and how impurities and water exposure affect these distributions, providing a deeper understanding of how these factors affect the magnetic properties of materials. In DoS & PDoS plots of Tc-MoS_2, Nb-MoS_2, Tc-W-MoS_2 and Nb-W-MoS_2, we found that the distributions of up-spin and down-spin electronic states near the Fermi level are asymmetrical. We determined the net magnetic moment arising from up-spin and down-spin of electrons in each orbital of the constituent atoms. Magnetic moment in the 4p, 4d & 5s orbitals of Mo atom have 0.03 µB /cell, 0.11 µB /cell & 0.00 µB /cell; 3s & 3p orbitals of S atoms have 0.00 µB /cell & 0.05 µB /cell; and 4p, 4d & 5s orbitals of Tc atom has -0.01 µ B /cell, -0.03 µB /cell & 0.00µB /cell values in Tc-MoS_2 material. Total magnetic moment of Tc-MoS_2 is found to be 0.15 µB /cell, and the magnetic moment based on integrated density of states (IDoS) is also estimated to be 0.15 µB /cell. The magnetic moment generated in Tc-MoS_2 is mainly due to the 4d orbital of Mo, 3p orbital of S, and 4d orbital of Tc atoms. Thus, Tc-MoS_2 is considered a magnetic material. The magnetic properties of Nb-MoS_2 are investigated by the analysis of its PDoS plot. It is determined that the 4p, 4d & 5s orbitals of Mo atoms contributed 0.01 µB /cell, 0.09 µB /cell, & 0.00 µB /cell magnetic moments respectively. Additionally, the magnetic moment carried out by 3s & 3p orbitals of S atoms have 0.00 µB /cell & 0.01 µB /cell; 4p, 4d & 5s orbitals of Nb atoms have -0.02 µB /cell, -0.08 µB /cell & 0.00 µB /cell respectively. Total magnetic moment of Nb-MoS_2 is found to be 0.01 µB /cell. The same value of magnetic moment of Nb-MoS_2 is determined by integrated density of states (IDoS) calculation. The dominant contribution of magnetic moment by 4d orbital of Mo, 3p orbital of S, and 4d orbital of Nb atoms in Nb-MoS_2. Hence, Nb-MoS_2 is a weak magnetic material.

Table 1: Bandgap energy (Eg), Fermi energy (Ef), Fermi energy shift (Es), total ground state energy (Et), and binding energy (Eb) of MoS_2, Tc-MoS_2, Nb-MoS_2, Tc-W-MoS_2, and Nb-W-MoS_2 materials.

Materials	Ef (eV)	Eg (eV)	Es (eV)	Et (Ry)	Eb (eV)
MoS_2	-1.89	1.80	-	-1741.61	6.83
Tc-MoS_2	-0.83	1.01	1.06	-1774.07	7.32
Nb-MoS_2	-2.26	1.10	-0.37	-1711.97	6.42
Tc-W-MoS_2	-1.01	1.13	0.88	-1810.08	7.89
Nb-W-MoS_2	-2.42	1.23	-0.53	-1747.98	6.98

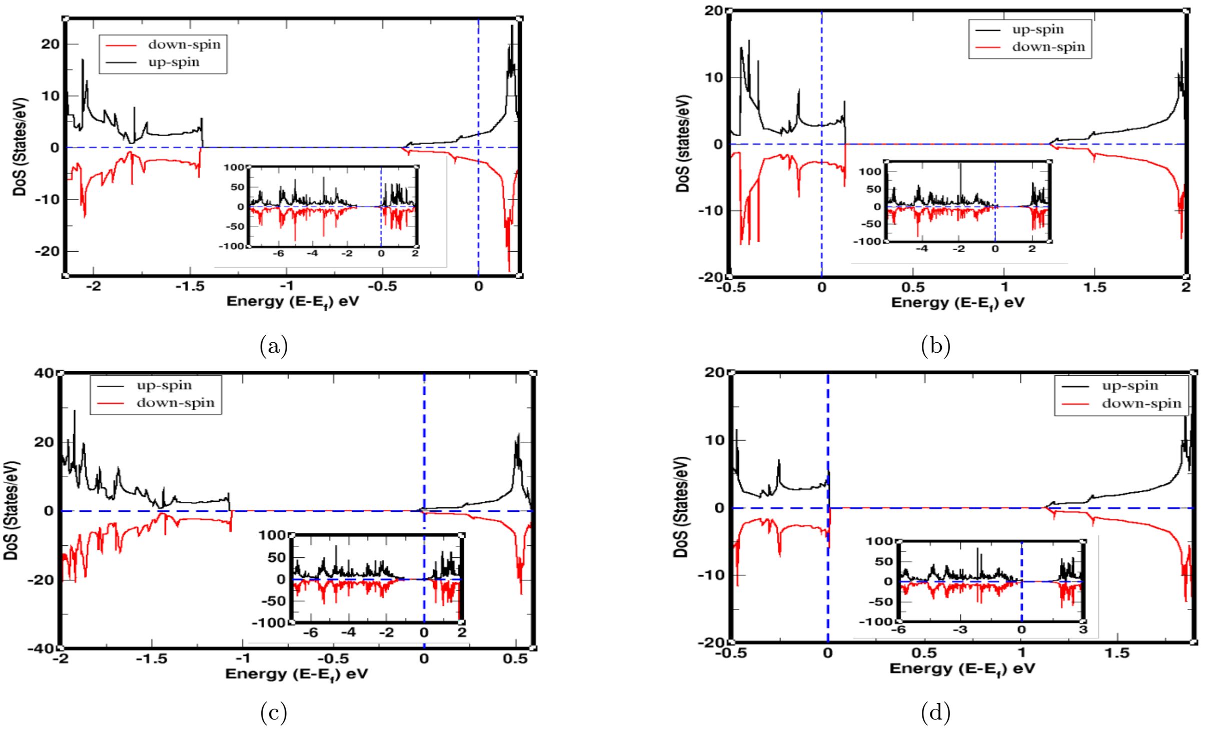

Figure 3: (Colour online) DoS plots of (a) Tc-MoS_2, (b) Nb-MoS_2, (c) Tc-W-MoS_2 and (d) Nb-W-MoS_2. In figures, horizontal dotted line separates the spin states, vertical dotted line indicates the Fermi level, and inset represents the DOS plots large range of energy level.

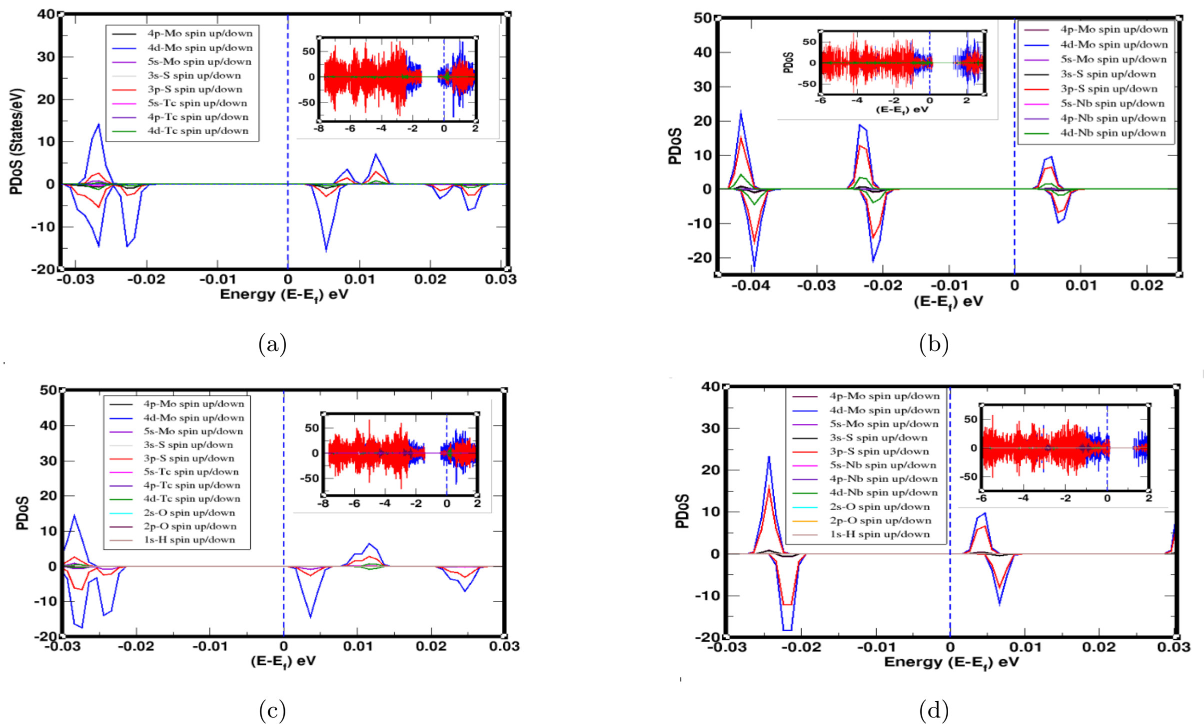

Figure 4: (Colour online) (a) PDoS plot of individual up-spin and down-spin states of electrons in the orbitals of Mo, S & Tc atoms of Tc-MoS^2 material, (b) PDoS plot of individual up-spin and down-spin states of electrons in the orbitals of Mo, S Nb atoms of Nb-MoS_2 material, (c) PDoS plot of individual up-spin and down-spin states of electrons in the orbitals of Mo, S, Tc, H O atoms of Tc-W-MoS_2 material, and (d) PDoS plot of individual up-spin and down-spin states of electrons in the orbitals of Mo, S, Nb, H & O atoms of Nb-W-MoS_2. In figures, horizontal dotted line separates the spin states, vertical dotted line indicates the Fermi level, and inset represents the PDoS plots of large-scale energy range.

Table 2: Total magnetic moment (μ) of Tc-MoS_2, Nb-MoS_2, Tc-W-MoS_2, and Nb-W-MoS_2 materials obtained by asymmetrically distributed up-spin and down-spin of electrons in various orbitals of different atoms.

Orbitals / Materials	Tc-MoS_2	Nb-MoS_2	Tc-W-MoS_2	Nb-W-MoS_2
μ of 4p-Mo	0.03	0.01	0.03	0.00
μ of 4d-Mo	0.11	0.09	0.12	0.08
μ of 5s-Mo	0.00	0.00	0.00	0.00
μ of 3s-S	0.00	0.00	0.00	0.00
μ of 3p-S	0.05	0.01	0.03	0.01
μ of 4p-Tc	-0.01	-	0.01	-
μ of 4d-Tc	-0.03	-	-0.04	-
μ of 5s-Tc	0.00	-	0.00	-
μ of 4p-Nb	-	-0.02	-	0.00
μ of 4d-Nb	-	-0.08	-	-0.07
μ of 5s-Nb	-	0.00	-	0.00
μ of 2s-O	-	-	0.00	0.00
μ of 2p-O	-	-	0.00	0.00
μ of 1s-H	-	-	0.00	0.00
Total (μ) μ_B/cell	0.15	0.01	0.15	0.02

Furthermore, we have estimated the magnetic properties of Tc-W-MoS2 and Nb-W-MoS2 materials by interpretating their PDoS plots. The magnetic properties of Tc-W-MoS_2 are predicted by the estimation of distributed electronic spin states in the individual orbital of each atom present in the structure. The 4p, 4d 5s orbitals of Mo atoms have magnetic moments 0.03 µB /cell, 0.12 µB /cell 0.00 µB /cell respectively in structure. Also, 3s 3p orbitals of S atoms have magnetic moments 0.00 µB /cell 0.03 µB /cell; and 4p, 4d 5s orbitals of Tc atom has magnetic moments 0.01 µB /cell, -0.04 µB /cell 0.00 µB /cell respectively. Similarly, we have estimated the magnetic moment generated by 2s 2p orbitals of O atom have values 0.00 µB /cell 0.00 µB /cell; and 1s orbital of H has value 0.00 µB /cell. The total magnetic moment of Tc-W-MoS_2 is obtained 0.15 µB /cell. We also have estimated the magnetic moment 0.15µ B /cell based on integrated density of states (IDoS). The magnetic moment in Tc-W-MoS_2 is mainly created by the dominant effect of 4d orbital of Mo, 3p orbital of S, and 4d orbital of Tc atoms. Therefore, Tc-W-MoS_2 is considered to be a magnetic material. In Nb-W-MoS_2 , the magnetic moment is observed in 4p, 4d, 5s orbitals of Mo atoms have 0.00 µB /cell, 0.08 µB /cell 0.00 µB /cell respectively. The magnetic moments given by 3s 3p orbitals of S atoms have values 0.00 µB /cell 0.00 µB /cell respectively. The 4p, 4d 5s orbitals of Nb atom has magnetic moments of 0.00 µB /cell, -0.07 µB /cell 0.00 µB /cell; and 2s & 2p orbitals of O has magnetic moments of 0.00 µB /cell 0.00 µB /cell, while the 1s orbital of H atom has a magnetic moment of value 0.00 µB /cell. The total magnetic moment of Nb-W-MoS_2 is found to be 0.02 µB /cell. Magnetic moment of Nb-W-MoS_2 also estimated through integrated density of states (IDoS), and found to be 0.02 µB /cell. The main source of magnetic moment in Nb-W-MoS_2 is 4d orbitals of Mo, 4d orbitals of Nb, and 3p orbital of S atoms in the structure. Thus, Nb-W-MoS_2 is weak a magnetic material. From the above calculations of magnetic moment in the materials, we found that impurity atoms on MoS_2 , and adsorbed water molecule on impurities defected MoS_2 intensified the magnetic properties in the materials. The detail calculations of magnetic moment of Tc-MoS_2 , Nb-MoS_2 , Tc-W-MoS_2 and Nb-W-MoS_2 materials by the analysis of individual electronic orbital of atoms are given in Table-2.

4 Conclusions

Structural, electronic, and magnetic properties of Tc-MoS_2, Nb-MoS_2, Tc-W-MoS_2 and Nb-W-MoS_2 materials have been explored by spin-polarized density functional theory (DFT) method with van der Waals (vdWs) corrections (DFT-D2) approach through computational tool Quantum ESPRESSO. It is found that Tc-MoS_2, Nb-MoS_2, Tc-W-MoS_2 and Nb-W-MoS_2 are stable materials. The nature of materials has been studied through their band structure and density of states (DoS) calculations, and the result showed that all materials have narrow bandgap semiconducting properties. The bandgap energy of Tc-MoS_2, Nb-MoS_2, Tc-W-MoS_2 and Nb-W-MoS_2 have values 1.01 eV, 1.10 eV, 1.15 eV and 1.23 eV respectively. The electronic band states of conduction band are appeared close to the Fermi energy level of Tc-MoS_2 Tc-W-MoS_2, and hence they are n-type semiconductor materials. On the other hand, band states of valence band are appeared near the Fermi energy level than the band states of conduction band in band structure and DoS plots of Nb-MoS_2 Nb-W-MoS_2 materials. It reflects that they have p-type semiconducting properties. The presence of impurities in MoS_2 and adsorbed water molecule on impurities defected MoS_2 affects the semiconducting behavior of pure MoS_2 by shifting the band states with respect to Fermi energy level. Band structure calculations and DoS analysis revealed that the impact of water molecules on the surface of MoS_2 can alter its electronic properties, leading to the creation of new energy levels and modifications to the bandgap, resulting in new electronic states. Magnetic properties of considered materials are studied on the basis of their density of states (DoS) and partial density of states (PDoS) calculations, and found that all materials have magnetic properties. Magnetic moment of materials is developed due to presence of unpair electronic spin states in the individual orbitals of atoms present in the material. The estimated magnetic moment of Tc-MoS_2, Nb-MoS_2, Tc-W-MoS_2 and Nb-W-MoS_2 have values 0.15 µB /cell, 0.01 µB /cell, 0.15 µB /cell 0.02 µB /cell respectively. The significant values of magnetic moment are given in materials due to the presence of unpaired spin state in the 4d orbitals of Mo atoms, 3p orbital of S atoms, and 4d orbitals of Tc Nb atoms. Hence, electronic and magnetic properties are enhanced in the materials due to the presence of impurity atoms on MoS_2 and adsorbed water molecule on impurities defected MoS_2.

References

[1] M. Chhowalla, H. S. Shin, G. Eda, L. J. Li, K. P. Loh, and H. Zhang. The chemistry of two-dimensional layered transition metal dichalcogenide nanosheets. *Nature Chemistry*, 5(4):263–275, 2013.

[2] C. Ataca, H. Sahin, and S. Ciraci. Stable, single-layer mx2 transition-metal oxides and dichalcogenides in a honeycomb-like structure. *The Journal of Physical Chemistry C*, 116(16):8983–8999, 2012.

[3] M. Bernardi, C. Ataca, M. Palummo, and J. C. Grossman. Optical and electronic properties of two-dimensional layered materials. *Nanophotonics*, 6(2):479–493, 2017.

[4] K. F. Mak, C. Lee, J. Hone, J. Shan, and T. F. Heinz. Atomically thin mos 2: a new direct-gap semiconductor. *Physical Review Letters*, 105(13):136805, 2010.

[5] S. Helveg, J. V. Lauritsen, E. Lægsgaard, I. Stensgaard, J. K. Norskov, B. S. Clausen, and F. Besenbacher. Atomic-scale structure of single-layer mos 2 nanoclusters. *Physical Review Letters*, 84(5):951, 2000.

[6] E. S. Kadantsev and P. Hawrylak. Electronic structure of a single mos2 monolayer. *Solid State Communications*, 152(10):909–913, 2012.

[7] C. V. Nguyen and N. N. Hieu. Effect of biaxial strain and external electric field on electronic properties of mos2 monolayer: A first-principles study. *Chemical Physics*, 468:9–14, 2016.

[8] H. K. Neupane and N. P. Adhikari. Electronic and magnetic properties of defected mos2 monolayer. *BIBECHANA*, 18(2):68–79, 2021.

[9] H. K. Neupane and N. P. Adhikari. Structural, electronic and magnetic properties of defected water adsorbed single-layer mos2. *Journal of Institute of Science and Technology*, 26(1):43–50, 2021.

[10] H. K. Neupane and N. P. Adhikari. Structural, electronic and magnetic properties of s sites vacancy defects graphene/mos2 van der waals heterostructures: First-principles study. *International Journal of Computational Materials Science and Engineering*, 10(02):2150009, 2021.

[11] L. M. Guiney, X. Wang, T. Xia, A. E. Nel, and M. C. Hersam. Assessing and mitigating the hazard potential of two-dimensional materials. *ACS Nano*, 12(7):6360–6377, 2018.

[12] A. Castellanos-Gomez. Why all the fuss about 2d semiconductors? *Nature Photonics*, 10(4):202–204, 2016.

[13] P. Samorì, V. Palermo, and X. Feng. Chemical approaches to 2d materials. *Advanced Materials*, 28(29):6027–6029, 2016.

[14] B. Radisavljevic, A. Radenovic, J. Brivio, V. Giacometti, and A. Kis. Single-layer mos2 transistors. *Nature Nanotechnology*, 6(3):147–150, 2011.

[15] D. Jena and A. Konar. Enhancement of carrier mobility in semiconductor nanostructures by dielectric engineering. *Physical Review Letters*, 98(13):136805, 2007.

[16] C. V. Nguyen. Tuning the electronic properties and schottky barrier height of the vertical graphene/mos2 heterostructure by an electric gating. *Superlattices And Microstructures*, 116:79–87, 2018.

[17] B. Radisavljevic, M. B. Whitwick, and A. Kis. Small-signal amplifier based on single-layer mos2. *Applied Physics Letters*, 101(4):043103, 2012.

[18] Y. Hu, M. Ruan, Z. Guo, R. Dong, J. Palmer, J. Hankinson, and W. A. De Heer. Structured epitaxial graphene: growth and properties. *Journal of Physics D: Applied Physics*, 45(15):154010, 2012.

[19] H. V. Phuc, N. N. Hieu, B. D. Hoi, L. T. Phuong, and C. V. Nguyen. First principles study on the electronic properties and schottky contact of graphene adsorbed on mos2 monolayer under applied out-plane strain. *Surface Science*, 668:23–28, 2018.

[20] C. Ataca and S. Ciraci. Functionalization of single-layer mos2 honeycomb structures. *The Journal of Physical Chemistry C*, 115(27):13303–13311, 2011.

[21] E. Scalise, M. Houssa, G. Pourtois, V. Afanas'ev, and A. Stesmans. Strain-induced semiconductor to metal transition in the two-dimensional honeycomb structure of mos2. *Nano Research*, 5(1):43–48, 2012.

[22] T. Heine. Transition metal chalcogenides: ultrathin inorganic materials with tunable electronic properties. *Accounts of Chemical Research*, 48(1):65–72, 2015.

[23] H. K. Neupane and N. P. Adhikari. Structural, electronic and magnetic properties of impurities defected graphene/mos2 van der waals heterostructure: first-principles study. *Journal of Nepal Physical Society*, 7(2):1–8, 2021.

[24] H. K. Neupane and N. P. Adhikari. Effect of vacancy defects in 2d vdw graphene/h-bn heterostructure: First-principles study. *AIP Advances*, 11(8), 2021.

[25] H. K. Neupane and N. P. Adhikari. Adsorption of water on c sites vacancy defected graphene/h-bn: First-principles study. *Journal of Molecular Modeling*, 28(4):107, 2022.

[26] L. M. Guiney, X. Wang, T. Xia, A. E. Nel, and M. C. Hersam. Assessing and mitigating the hazard potential of two-dimensional materials. *ACS Nano*, 12(7):6360–6377, 2018.

[27] H. K. Neupane and N. P. Adhikari. Adsorption of water molecule in graphene/mos2 heterostructure with vacancy defects in mo sites. *Advances in Condensed Matter Physics*, 2022.

[28] J. Kibsgaard, J. V. Lauritsen, E. Lægsgaard, B. S. Clausen, H. Topsøe, and F. Besenbacher. Cluster support interactions and morphology of mos2 nanoclusters in a graphite-supported hydrotreating model catalyst. *Journal of the American Chemical Society*, 128(42):13950–13958, 2006.

[29] M. R. Uhlig, D. Martin-Jimenez, and R. Garcia. Atomic-scale mapping of hydrophobic layers on graphene and few-layer mos2 and wse2 in water. *Nature Communications*, 10(1):1–7, 2019.

[30] Q. Li, J. Song, F. Besenbacher, and M. Dong. Two-dimensional material confined water. *Accounts of Chemical Research*, 48(1):119–127, 2015.

[31] D. Sarkar, W. Liu, X. Xie, A. C. Anselmo, S. Mitragotri, and K. Banerjee. Mos2 field-effect transistor for next-generation label-free biosensors. *ACS Nano*, 8(4):3992–4003, 2014.

[32] H. K. Neupane and N. P. Adhikari. First-principles study of structure, electronic, and magnetic properties of c sites vacancy defects in water adsorbed graphene/mos 2 van der waals heterostructures. *Journal of Molecular Modeling*, 27:1–12, 2021.

[33] M. Bernardi, C. Ataca, M. Palummo, and J. C. Grossman. Optical and electronic properties of two-dimensional layered materials. *Nanophotonics*, 6(2):479–493, 2017.

[34] S. Tongay, J. Suh, C. Ataca, W. Fan, A. Luce, J. S. Kang, and J. Wu. Defects activated photoluminescence in two-dimensional semiconductors: interplay between bound, charged and free excitons. *Scientific Reports*, 3(1):1–5, 2013.

[35] G. Levita, P. Restuccia, and M. C. Righi. Graphene and mos2 interacting with water: A comparison by ab initio calculations. *Carbon*, 107:878–884, 2016.

[36] M. R. Vazirisereshk, A. Martini, D. A. Strubbe, and M. Z. Baykara. Solid lubrication with mos2: a review. *Lubricants*, 7(7):57, 2019.

[37] Z. Li and et al. Effect of airborne contaminants on the wettability of supported graphene and graphite. *Nature Materials*, 12:925–931, 2013.

[38] A. K. Singh, P. Kumar, D. J. Late, A. Kumar, S. Patel, and J. Singh. 2d layered transition metal dichalcogenides (mos2): synthesis, applications and theoretical aspects. *Applied Materials Today*, 13:242–270, 2018.

[39] C. Kittel, P. McEuen, and P. McEuen. *Introduction to Solid State Physics*. Wiley, 1996.

[40] J. Maier. Defect chemistry: composition, transport, and reactions in the solid state; part i: thermodynamics. *Angewandte Chemie International Edition in English*, 32(3):313–335, 1993.

[41] H. K. Neupane and N. P. Adhikari. Structure, electronic and magnetic properties of 2d graphene-molybdenum disulphide (g-mos2) heterostructure (hs) with vacancy defects at mo sites. *Computational Condensed Matter*, 24:e00489, 2020.

[42] H. K. Neupane and N. P. Adhikari. Structural, electronic and magnetic properties of s sites vacancy defects graphene/mos2 van der waals heterostructures: First-principles study. *International Journal of Computational Materials Science and Engineering*, 10(02):2150009, 2021.

[43] M. V. Makarova, Y. Akaishi, T. Ikarashi, K. S. Rao, S. Yoshimura, and H. Saito. Alternating magnetic force microscopy: Effect of si doping on the temporal performance degradation of amorphous fecob magnetic tips. *Journal of Magnetism and Magnetic Materials*, 471:209–214, 2019.

[44] P. Hohenberg and W. Kohn. Inhomogeneous electron gas. *Physical Review*, 136(3B):B864, 1964.

[45] P. Giannozzi, S. Baroni, N. Bonini, M. Calandra, R. Car, C. Cavazzoni, and R. M. Wentzcovitch. Quantum espresso: a modular and open-source software project for quantum simulations of materials. *Journal of Physics: Condensed Matter*, 21(39):395502, 2009.

[46] S. Grimme. Accurate description of van der waals complexes by density functional theory including empirical corrections. *Journal of Computational Chemistry*, 25(12):1463–1473, 2004.

[47] J. P. Perdew, K. Burke, and M. Ernzerhof. Generalized gradient approximation made simple. *Physical Review Letters*, 77(18):3865, 1996.

[48] R. M. Martin. *Electronic Structure: Basic Theory and Practical Methods.* Cambridge University Press, 2020.

[49] H. J. Monkhorst and J. D. Pack. Special points for brillouin-zone integrations. *Physical Review B*, 13(12):5188, 1976.

[50] B. G. Pfrommer, M. Cote, S. G. Louie, and M. L. Cohen. Relaxation of crystals with the quasi-newton method. *Journal of Computational Physics*, 131(1):233–240, 1997.

[51] N. Marzari, D. Vanderbilt, A. De Vita, and M. C. Payne. Thermal contraction and disordering of the al (110) surface. *Physical Review Letters*, 82(16):3296, 1999.

[52] N. Pantha, K. Belbase, and N. P. Adhikari. First-principles study of the interaction of hydrogen molecular on na-adsorbed graphene. *Applied Nanoscience*, 5(4):393–402, 2015.

[53] B. Oli, C. Bhattarai, B. Nepal, and N. Adhikari. First-principles study of adsorption of alkali metals (li, na, k) on graphene. *Advanced Nanomaterials and Nanotechnology*, page 515–529, 2013.